# Supplementary Information for:

# Surface curvature effects in neutral and protonated water clusters: insights from DFT and energy decomposition analysis†

Murillo H. Queiroz[ab], Bruno S. Sampaio[a], Celine Nieuwland[b], Célia Fonseca Guerra[b], Tiago V. Alves[a], Roberto Rivelino*[c]

[a] Departamento de Físico-Química, Instituto de Química, Universidade Federal da Bahia Rua Barão de Jeremoabo, 147, 40170-115, Salvador, Bahia, Brazil

[b] Department of Chemistry and Pharmaceutical Sciences, Amsterdam Institute for Molecular and Life Sciences (AIMMS), Vrije Universiteit Amsterdam, De Boelelaan 1108, 1081 HZ Amsterdam, The Netherlands

[c] Instituto de Física, Universidade Federal da Bahia, 40210-340 Salvador, Bahia, Brazil

*Corresponding authors. E-mail: rivelino@ufba.br

## Voronoi Deformation Density (VDD) Charge Analysis for Complexes

The VDD method[62] provides a way to assess how electron density is redistributed upon complex formation. In this context, the change in atomic charge ($\Delta Q_A$) for a given atom A in fragment *i* is obtained by integrating the deformation density over the Voronoi cell of atom A. This deformation density is defined as the difference between the total electron density of the complex, $\rho$(r), and the sum of the densities of the isolated fragments, $\sum_{fragment,i} \rho_i(r)$:

$$\Delta Q_A = -\int_{Voronoi\ cell\ of\ A\ in\ the\ complex} \left[ \rho(r) - \sum_{fragment,i} \rho_i(r) \right]$$

This analysis shows how the interaction between fragments alters the local electron density around atom A. Summing $\Delta Q_A$ over all atoms in fragment *i* gives the total charge transfer associated with that fragment: a negative value ($\Delta Q_{\mathrm{fragment,i}} < 0$) indicates net electron gain, while a positive value ($\Delta Q_{\mathrm{fragment,i}} > 0$) indicates net electron loss due to complex formation.

$$\Delta Q_{fragment,i} = \sum_{A\ in\ fragment} \Delta Q_A$$

## Non-Covalent Interactions

Non-Covalent Interactions (NCI)[S1] plots are based on the gradients of electron density are provided to identify and visualize weak interactions through color-coded isosurfaces.

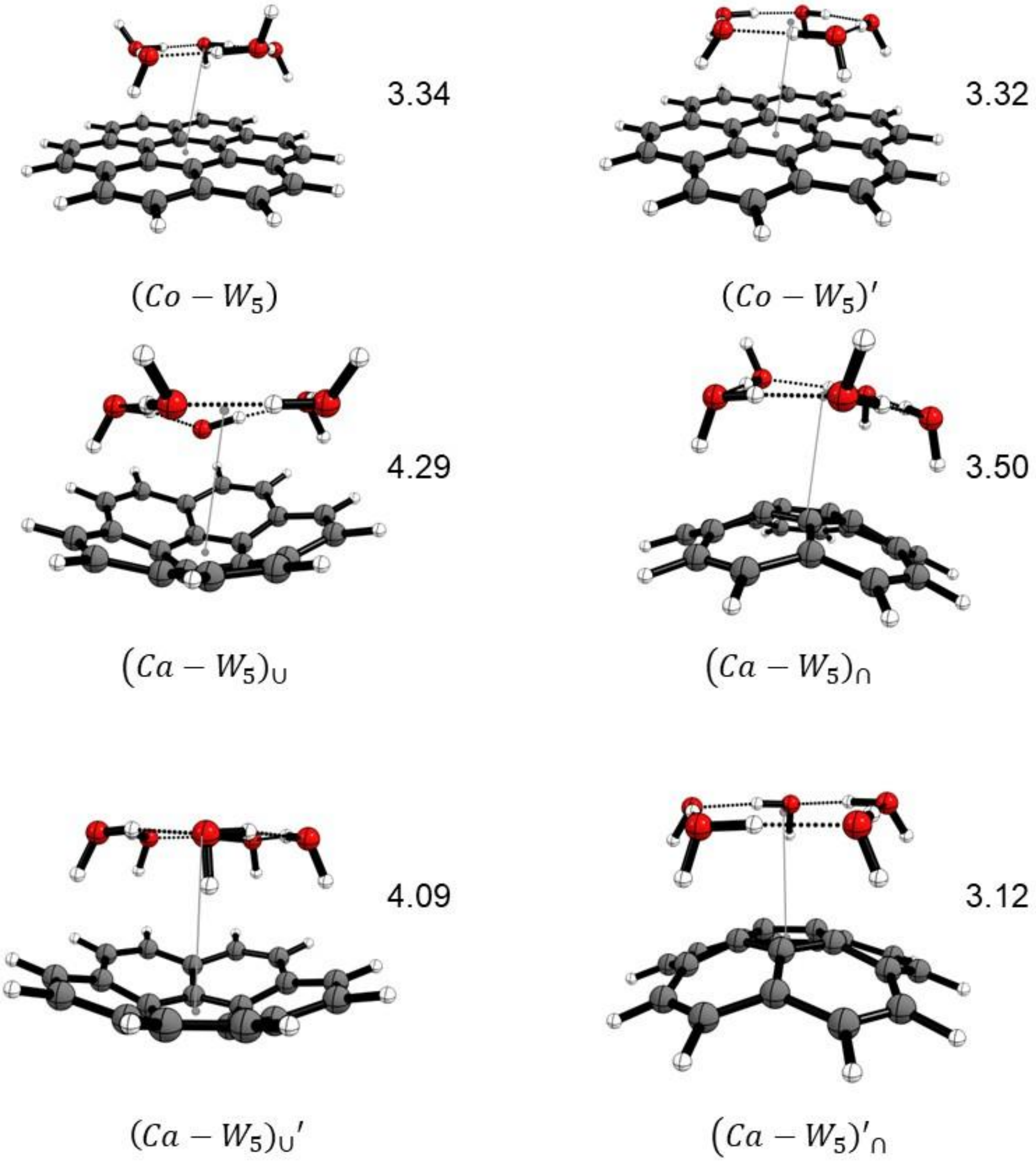

$(Co - W_5)$

$(Co - W_5)'$

$(Ca - W_5)_{\cup}$

$(Ca - W_5)_{\cap}$

$(Ca - W_5)_{\cup}'$

$(Ca - W_5)'_{\cap}$

**Figure S1**. B3LYP-D3(BJ)/def2-TZVP optimized structures of the neutral water cluster–PAH complexes. Values in black are the intercluster distances ($Co/Ca\cdots W_5$) in Å.

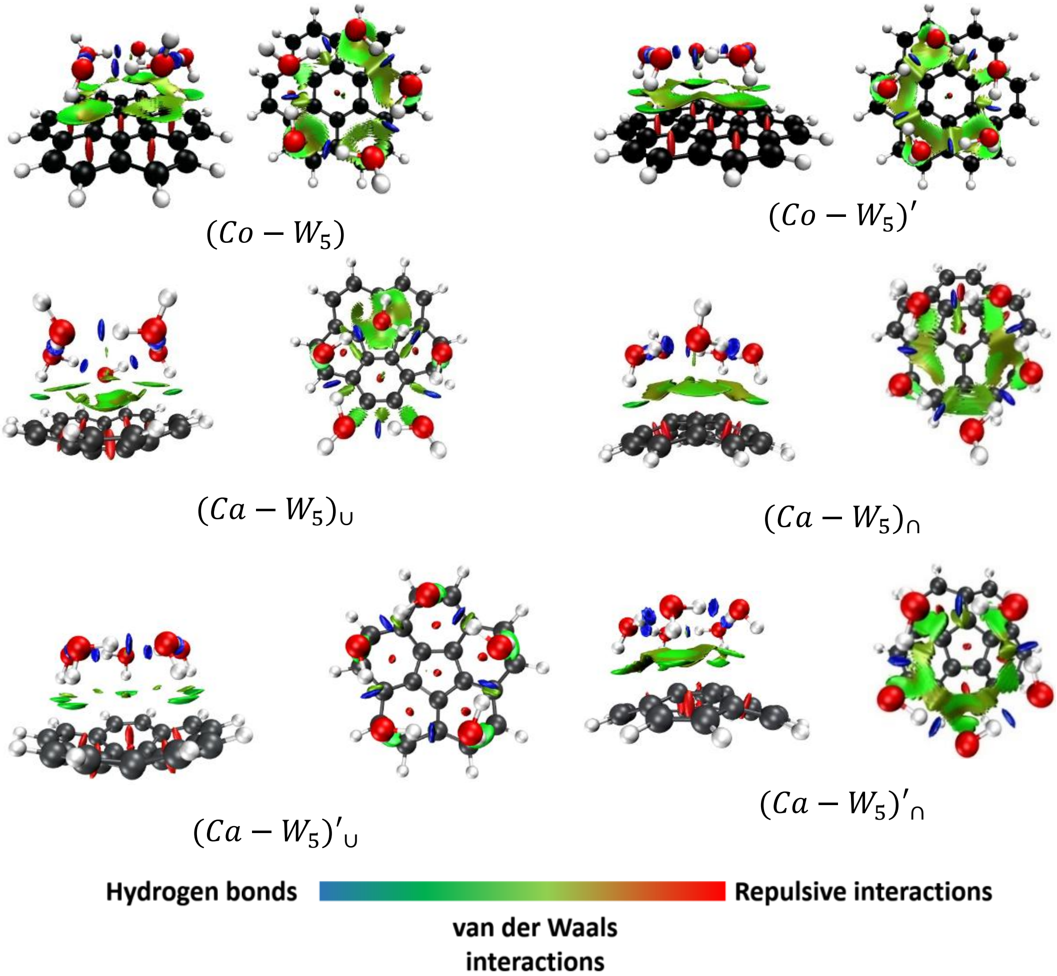

$(Co-W_5)$

$(Co-W_5)'$

$(Ca-W_5)_\cup$

$(Ca-W_5)_\cap$

$(Ca-W_5)'_\cup$

$(Ca-W_5)'_\cap$

**Figure S2**. Optimized structures and NCI analysis for the neutral complexes involving water pentamers and corannulene. Blue, green, and red electron density regions denote conventional H-bonds, dispersion, and repulsive interactions, respectively (reduced densities isovalue contours value = 0.5). We display side view (left) and top view (right) of each complex for clarity.

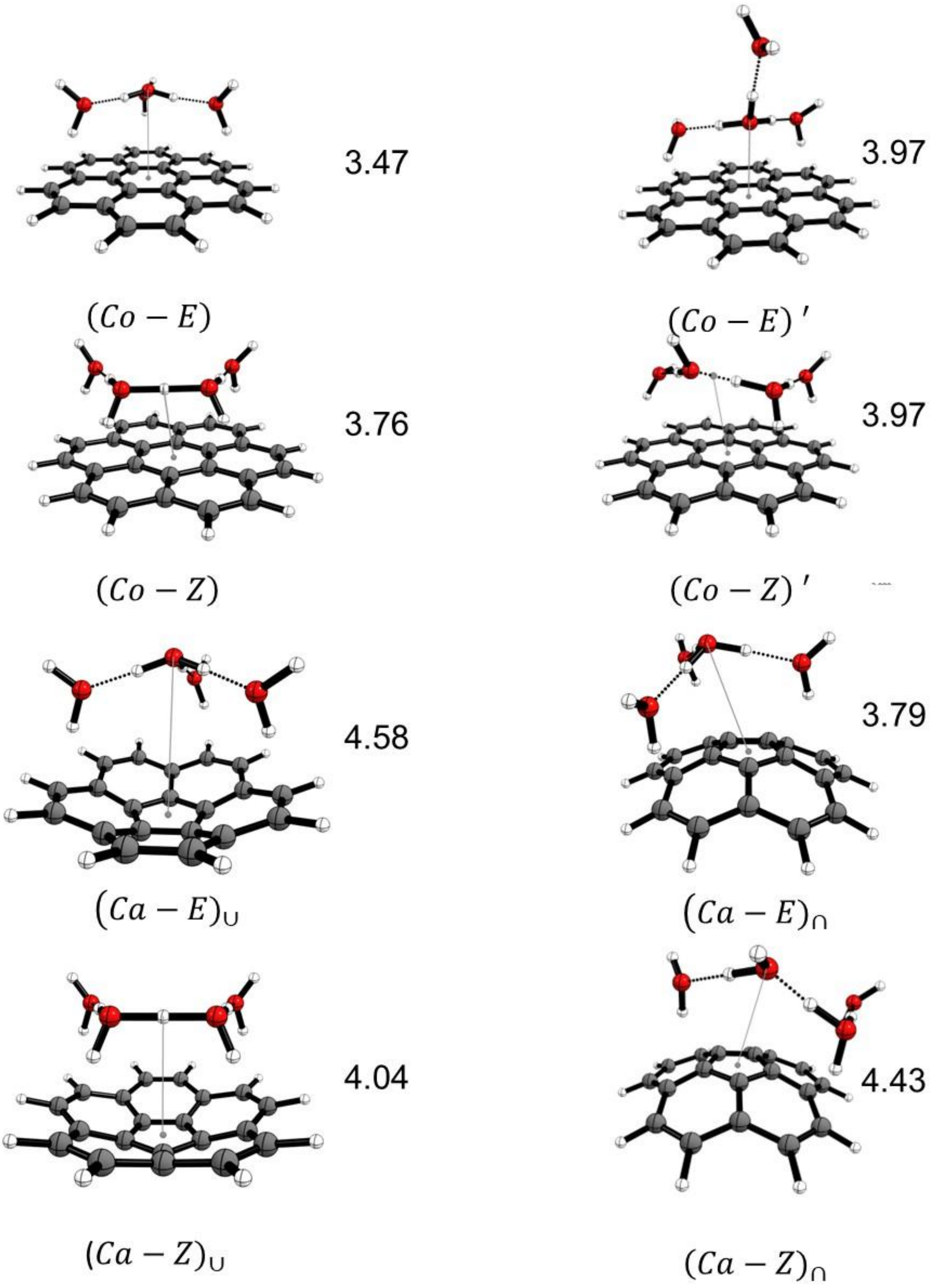

$(Co-E)$ $(Co-E)'$

$(Co-Z)$ $(Co-Z)'$

$(Ca-E)_{\cup}$ $(Ca-E)_{\cap}$

$(Ca-Z)_{\cup}$ $(Ca-Z)_{\cap}$

**Figure S3**. Some optimized structures of the cationic water cluster–PAH complexes with B3LYP-D3(BJ)/def2-TZVP. Values in black are the interclusters (*Co*/*Ca*···*E*/*Z*) distances in Å.

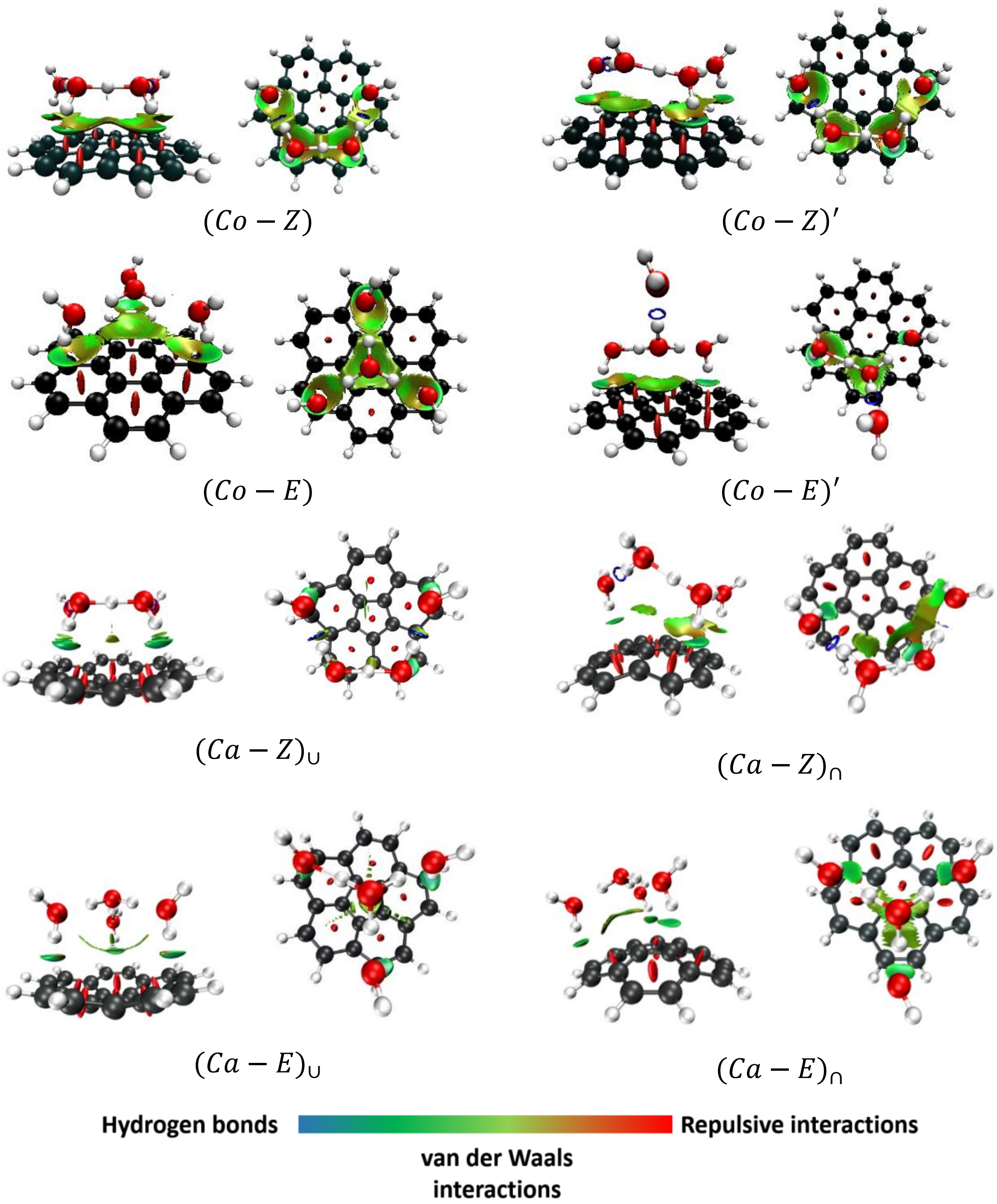

$(Co-Z)$ $(Co-Z)'$

$(Co-E)$ $(Co-E)'$

$(Ca-Z)_{\cup}$ $(Ca-Z)_{\cap}$

$(Ca-E)_{\cup}$ $(Ca-E)_{\cap}$

**Figure S4**. Some optimized structures with B3LYP-D3(BJ)/def2-TZVP and NCI analysis for the complexes involving Zundel and Eigen cations. Green and red electron density regions denote dispersion and repulsive interactions, respectively (reduced densities isovalue contours value = 0.5). We display side view (left) and top view (right) of each complex for clarity.

**Table S1**. Bond, interaction, and strain energies (in kcal mol$^{-1}$) of the neutral water cluster–PAH complexes calculated at M06-2X/TZ2P.[a]

| System | $\Delta E_{bond}{}^{a}$ | $\Delta E_{int}$ | $\Delta E_{strain}{}^{b}$ | $\Delta E^{PAH}_{strain}$ | $\Delta E^{W_5}_{strain}$ |
|---|---|---|---|---|---|
| $(Co - W_5)$ | –10.6 | –11.2 | 0.6 | 0.3 | 0.3 |
| $(Co - W_5)'$ | –10.9 | –14.5 | 3.6 | 0.3 | 3.3 |
| $(Ca - W_5)_{\cup}$ | –9.1 | –11.5 | 2.5 | 0.4 | 2.1 |
| $(Ca - W_5)_{\cap}$ | –8.2 | –8.9 | 0.7 | 0.3 | 0.4 |
| $(Ca - W_5)'_{\cup}$ | –6.5 | –12.1 | 5.6 | 0.2 | 5.4 |
| $(Ca - W_5)'_{\cap}$ | –7.2 | –11.5 | 4.3 | 0.6 | 3.7 |

[a] $\Delta E_{bond} = \Delta E_{strain} + \Delta E_{int}$ [b] $\Delta E_{strain} = \Delta E^{PAH}_{strain} + \Delta E^{W_5}_{strain}$

**Table S2**. EDA components (in kcal mol$^{-1}$) for the neutral water cluster–PAH complexes calculated at M06-2X/TZ2P.[a]

| System | $\Delta E_{\mathrm{int}}$ | $\Delta V_{\mathrm{elstat}}$ | $\Delta E_{\mathrm{Pauli}}$ | $\Delta E_{\mathrm{oi}}$ |
|---|---|---|---|---|
| $(Co - W_5)$ | –11.2 | –9.5 | 4.9 | –6.5 |
| $(Co - W_5)'$ | –14.5 | –13.2 | 5.9 | –7.3 |
| $(Ca - W_5)_{\cup}$ | –11.5 | –11.6 | 6.3 | –6.1 |
| $(Ca - W_5)_{\cap}$ | –8.9 | –8.4 | 4.6 | –5.1 |
| $(Ca - W_5)'_{\cup}$ | –12.1 | –14.0 | 10.3 | –8.4 |
| $(Ca - W_5)'_{\cap}$ | –11.5 | –11.8 | 5.2 | –5.0 |

[a] $\Delta E_{\mathrm{int}} = \Delta V_{\mathrm{elstat}} + \Delta E_{\mathrm{Pauli}} + \Delta E_{\mathrm{oi}}$

**Table S3**. Bond, interaction, and strain energies (in kcal mol$^{-1}$) of the cationic water cluster–PAH complexes calculated at M06-2X/TZ2P.

| System | $\Delta E_{bond}{}^{a}$ | $\Delta E_{int}$ | $\Delta E_{strain}{}^{b}$ | $\Delta E^{PAH}_{strain}$ | $\Delta E^{Z/E}_{strain}$ |
|---|---|---|---|---|---|
| $(Co - E)$ | –24.8 | –25.8 | 1.0 | 0.1 | 0.9 |
| $(Co - Z)$ | –26.4 | –29.4 | 2.9 | 0.2 | 2.7 |
| $(Ca - Z)_{\cup}$ | –20.3 | –24.9 | 4.6 | 0.8 | 3.8 |
| $(Ca - Z)_{\cap}$ | –21.6 | –23.9 | 2.3 | 0.1 | 2.2 |
| $(Ca - E)_{\cup}$ | –17.1 | –19.4 | 2.2 | 0.5 | 1.7 |
| $(Ca - E)_{\cap}$ | –22.4 | –24.3 | 2.0 | 0.2 | 1.8 |

[a] $\Delta E_{bond} = E_{\mathrm{PAH-Z/E}} - E_{\mathrm{PAH}} - E_{\mathrm{Z/E}}$ (Note that the bonding energy of each cationic complex is computed with respect to the Eigen or Zundel cation). [b] $\Delta E_{strain} = \Delta E^{PAH}_{strain} + \Delta E^{Z/E}_{strain}$

**Table S4**. EDA components (in kcal mol$^{-1}$) for the neutral water cluster–PAH complexes calculated at M06-2X/TZ2P.[a]

| System | $\Delta E_{\text{int}}$ | $\Delta V_{\text{elstat}}$ | $\Delta E_{\text{Pauli}}$ | $\Delta E_{\text{oi}}$ |
|---|---|---|---|---|
| $(Co-E)$ | –25.8 | –17.5 | 9.1 | –17.3 |
| $(Co-Z)$ | –29.4 | –19.8 | 10.3 | –19.8 |
| $(Ca-Z)_{\cup}$ | –24.9 | –19.2 | 15.4 | –21.1 |
| $(Ca-Z)_{\cap}$ | –23.9 | –16.5 | 8.8 | –16.2 |
| $(Ca-E)_{\cup}$ | –19.4 | –14.6 | 12.4 | –17.1 |
| $(Ca-E)_{\cap}$ | –24.3 | –17.0 | 9.3 | –16.6 |

[a] $\Delta E_{\text{int}} = \Delta V_{\text{elstat}} + \Delta E_{\text{Pauli}} + \Delta E_{\text{oi}}$

**Table S5**. Calculated lower-frequency vibrational modes (in cm$^{-1}$) of the Eigen cation.

| Mode | This work | MCTDH[a] | Expt. 1[b] | Expt. 2[c] |
|---|---|---|---|---|
| Global $O_4$ pyramidalization | 66.2 | 60 | - | - |
| Water ligand wagging | 242.9 | 240 | - | 236 |
| O-O stretching | 279.5 | 310 | - | 316 |
| Water ligand rocking | 343.8 | 370 | - | - |
| Hydronium wagging | 990.8 | 920 | - | 894 |
| Hydronium umbrella | 1165.9 | 970 | - | 1014 |
| OH-bend water ligands | 1637.4 | 1620 | 1615 | 1615 |
| Hydronium O-H stretch | 2974.0 | 2670 | 2653 | - |
| Symmetric OH-stretch water ligands | 3779.0 | 3670 | 3636 | - |
| Asymmetric OH-stretch water ligands | 3870.7 | 3800 | 3724 | - |

[a] Simulations from ref. 72 in the main manuscript; [b] experimental data from supplementary ref. [2]; and [c] Experimental data from supplementary ref. [3]

**Table S6**. Calculated fundamentals (in cm$^{-1}$) of the Zundel/Eigen complexes with coronene and corannulene in comparison with the isolated cations. The shifts are given in parentheses.

| Assignment | $E$ | $(Co-E)$ | $(Co-E')$ |
|---|---|---|---|
| Hydronium umbrella | 1166.0 | 1117.2 (–48.8) | 1229.9 (63.9) |
| Hydronium + 2$H_2O$ bending | 1623.1 | 1606.5 (–16.6) | 1612.1 (–11.0) |
| Hydronium + 2$H_2O$ bending | 1623.3 | 1606.9 (–16.4) | 1616.3 (–7.0) |
| Water ligand O-H bending | 1637.4 | 1627.2 (–10.2) | 1631.8 (–5.6) |
| Hydronium bending | 1687.5 | 1687.6 (0.1) | 1707.0 (19.5) |
| Hydronium bending | 1688.0 | 1688.8 (0.8) | 1741.3 (53.3) |
| Hydronium asym. O-H stretching | 2839.4 | 2759.9 (–79.5) | 2551.4 (–288.0) |
| Hydronium asym. O-H stretching | 2839.7 | 2764.1 (–75.6) | 2747.3 (-92.4) |
| Hydronium sym. O-H stretching | 2974.0 | 2918.7 (–55.3) | 3082.0 (108.0) |
| Assignment | $E$ | $(Ca-E)_\cup$ | $(Ca-E)_\cap$ |
| Hydronium umbrella | 1166.0 | 1297.9 (+131.9) | 1284.0 (+118.0) |
| Hydronium + 2$H_2O$ bending | 1623.1 | 1610.6 (–12.7) | 1594.3 (–28.8) |
| Hydronium + 2$H_2O$ bending | 1623.3 | 1623.3 (0.0) | 1618.7 (–4.6) |
| Water ligand O-H bending | 1637.4 | 1620.0 (–1.5) | 1603.2 (–34.2) |
| Hydronium bending | 1687.5 | 1680.1 (–7.4) | 1706.8 (+19.3) |
| Hydronium bending | 1688.0 | 1716.3 (+28.3) | 1712.9 (+24.9) |
| Hydronium asym. O-H stretching | 2839.4 | 2710.1 (–129.3) | 2728.3 (–111.1) |
| Hydronium asym. O-H stretching | 2839.7 | 2743.3 (–96.4) | 2780.7 (–59.4) |
| Hydronium sym. O-H stretching | 2974.0 | 2933.1 (–40.9) | 2952.2 (–18.8) |
| Assignment | $Z$ | $(Co-Z)$ | $(Co-Z')$ |
| $H_2O\cdots H^+\cdots OH_2$ bending | 908.4 | 942.1 (33.7) | 948.3 (39.9) |
| $H_2O\cdots H^+\cdots OH_2$ bending | 999.6 | - | - |
| $H_2O\cdots H^+\cdots OH_2$ bending | 1058.5 | 1073.3 (14.8) | 1030.7 (–27.8) |
| $H_2O\cdots H^+\cdots OH_2$ bending | 1416.0 | 1287.0 (–129.0) | 1388.3 (–27.7) |
| $H_2O\cdots H^+\cdots OH_2$ bending | 1581.9 | - | 1613.3 (31.4) |
| Water ligand bending | 1633.0 | 1611.6 (–21.4) | 1627.1 (–5.9) |
| Water ligand bending | 1636.5 | 1626.7 (–9.8) | 1634.9 (–1.6) |
| Shared-proton + 2$H_2O$ bending | 1697.8 | 1685.8 (–12.0) | 1722.7 (24.9) |
| Shared-proton + 2$H_2O$ bending | 1747.3 | 1715.1 (–32.2) | 1865.9 (118.6) |
| H-bonded sym. O-H stretching | 2992.5 | 3002.0 (9.5) | 2782.8 (–209.7) |
| H-bonded asym. O-H stretching | 3033.3 | 3039.7 (6.4) | 3137.7 (104.4) |
| Assignment | $Z$ | $(Ca-Z)_\cup$ | $(Ca-Z)_\cap$ |
| $H_2O\cdots H^+\cdots OH_2$ bending | 908.4 | 928.8 | 950.0* |
| $H_2O\cdots H^+\cdots OH_2$ bending | 999.6 | - | 950.4 |
| $H_2O\cdots H^+\cdots OH_2$ bending | 1058.5 | - | 1010.9 |
| $H_2O\cdots H^+\cdots OH_2$ stretching | - | 939.2 | - |
| $H_2O\cdots H^+\cdots OH_2$ stretching | - | 1072.9 | - |
| $H_2O\cdots H^+\cdots OH_2$ bending | 1416.0 | 1302.4 | 1402.8 |
| $H_2O\cdots H^+\cdots OH_2$ bending | 1581.9 | - | 1448.5 |
| Water ligand bending | 1633.0 | 1613.6 | 1611.5 |
| Water ligand bending | 1636.5 | 1613.6 | 1619.8 |
| Shared-proton + 2$H_2O$ bending | 1697.8 | 1694.5 (–3.3) | 1708.3 (+10.5) |
| Shared-proton + 2$H_2O$ bending | 1747.3 | 1714.0 (–33.3) | 1792.3 (+45.0) |
| $H_2O\cdots H^+\cdots OH_2$ bending | - | 1804.2 | - |
| H-bonded sym. O-H stretching | 2992.5 | 3043.3 (+50.8) | 3097.8 (+105.3) |
| H-bonded asym. O-H stretching | 3033.3 | 3012.7 (–20.6) | 2873.6 (–159.7) |

* Resonance with torsional motion of corannulene.

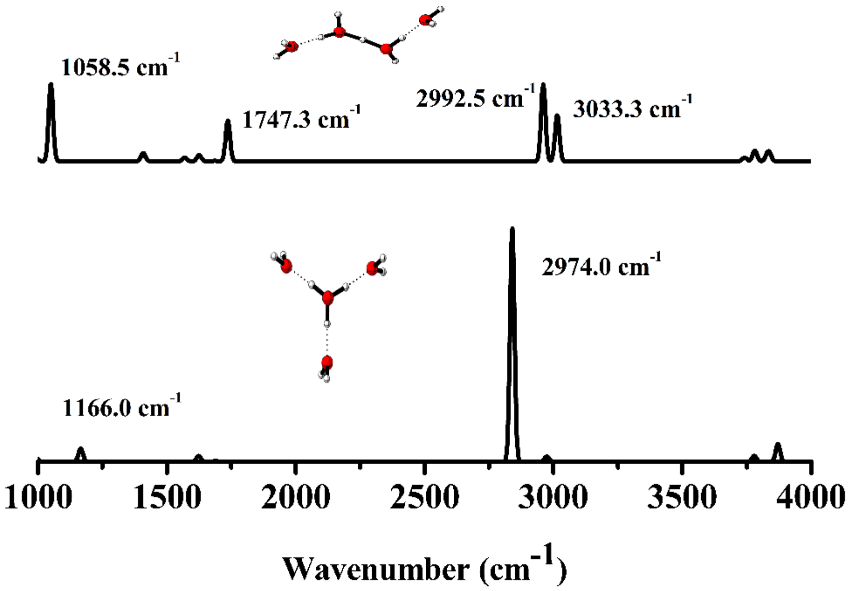

**Figure S5.** Calculated IR spectra of the isolated Zundel (top) and Eigen cations (bottom).

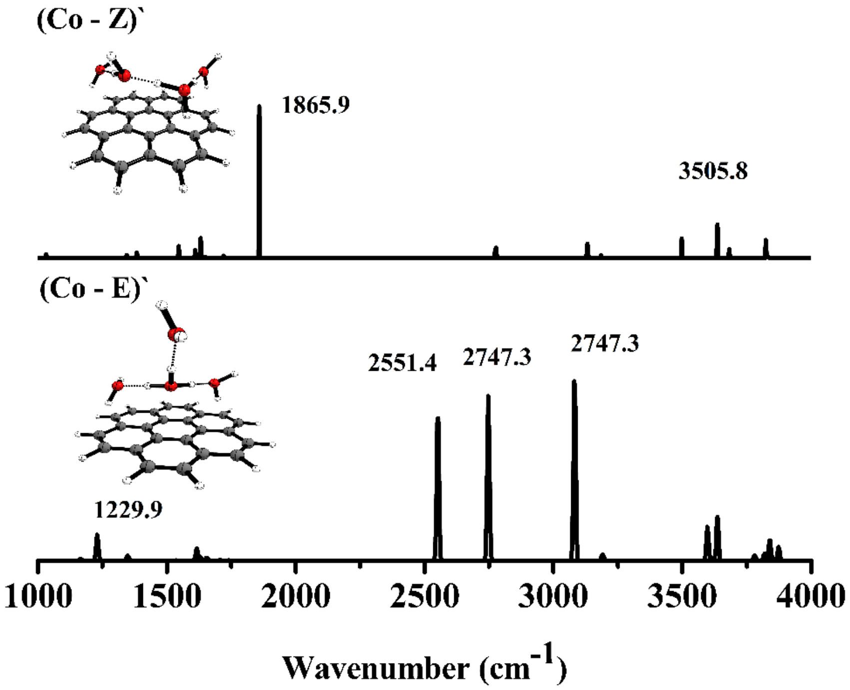

**Figure S6.** Calculated IR spectra of the $(Co - Z)'$ (top) and $(Co - E)'$ cations (bottom).

## Supplementary references

S1. E. R. Johnson, S. Keinan, P. Mori-Sánchez, J. Contreras-García, A. J. Cohen and W. Yang, *J. Am. Chem. Soc.*, **2010**, *132*, 6498–6506.

S2 C. T. Wolke, J. A. Fournier, L. C. Dzugan, M. R. Fagiani, T. T. Odbadrakh, H. Knorke, K. D. Jordan, A. B. McCoy, K. R. Asmis and M. A. Johnson, *Science*, **2016**, *354*, 1131–1135.

S3 T. K. Esser, H. Knorke, K. R. Asmis, W. Schöllkopf, Q. Yu, C. Qu, J. M. Bowman and M. Kaledin, *J. Phys. Chem. Lett.*, **2018**, *9*, 798–803.